New insights on the release and self-healing model of stimuli-sensitive liposomes

Olga Zaborova, Vadim Timoshenko, Corinne Nardin, Sergey Filippov

New insights on the release and self-healing model of stimuli-sensitive liposomes

Olga V. Zaborova[a], Vadim A. Timoshenko[a], Corine Nardin[b], Sergey K. Fillipov[c,*]

[a] *Chemistry Department, Moscow State University, Leninskie gory 1-3, Moscow, 119991, Russian Federation*
[b] *Universite de Pau et des Pays de l'Adour, E2S UPPA, CNRS, IPREM, Pau, 64053, France*
[c] *School of Pharmacy, University of Reading, Whiteknights, Reading, RG6 6AD, Berkshire, United Kingdom*

Abstract

The mixing of conventional and pH-sensitive lipids was exploited to design novel stimuli-responsive liposomes (fliposomes) that could be used for smart drug delivery. We deeply investigated the structural properties of the fliposomes and revealed the mechanisms that are involved in a membrane transformation during a pH change. From ITC experiments we observed the existence of a slow process that was attributed to lipid layers arrangement with changing pH. Moreover, we determined for the first time the pKa value of the trigger-lipid in an aqueous milieu that is drastically different from the methanol-based values reported previously in the literature. Furthermore, we studied the release kinetics of encapsulated NaCl and proposed a novel model of release that involves the physical fitting parameters that could be extracted from the release curves fitting. We have obtained for the first time, the values of pores self-healing times and were able to trace their evolution with changing pH, temperature, the amount of lipid-trigger.

Keywords: fliposomes, SAXS, trigger lipid, liposomes, drug delivery, smart materials

*Corresponding author at School of Pharmacy, University of Reading, United Kingdom
Email address: sfill225@gmail.com (Sergey K. Fillipov)

1. Introduction

Drug delivery is a rapidly developing field in pharmacy. However, this development is severely hampered by the fact that most of active substances in medicine are poorly soluble in water [1], thus emphasizing the importance of the choice of an appropriate drug delivery excipient [2].

Liposomes, spherical lipid bilayer vesicles, have been used as containers for the delivery of biologically active substances for a long time [3, 4, 5]. Due to the unique liposomal structure one can incorporate either hydrophilic substances into the internal cavity of liposomes, or hydrophobic — into the area of lipids acyl tails [6]. Despite considerable progress in the field of liposomal containers, quite a few liposomal drugs are available on the market now due to a number of severe drawbacks of such containers. Low therapeutic effect of liposomal drugs or low capture efficiency of liposomes by the target cells is among them [7].

Based on this knowledge, recent research is focused on improving the liposomal drugs therapeutic effect by fulfilling the targeted release of the encapsulated drug in response to the microenvironment change in a pathogenic tissue [8]. It is known that inflammation and some tumors have a weakly acidic medium (pH 5.5–6.9) in comparison to healthy tissues (pH 7.4)[9], so the containers which are capable of contents release in response to the decrease in pH are of special interest [10, 11, 12, 13, 14, 15].

Recently the new class of lipid-like pH-responsive compounds based on trans-2-morpholinocyclohexanol was described [16]. Such lipid-like compounds undergo conformational flip after protonation due to formation of a hydrogen bond between morpholine and hydroxyl substitutes in cyclohexanol ring [17, 18]. The term “fliposomes” was suggested to be used for liposomes containing such pH-triggerable lipid.

The “fliposomes”-based approach was successfully applied previously to design a multiliposomal container made of polycationic particles and anionic fliposomes [19]. In this study the propensity of anionic fliposomes, individual or complexed with polycationic particles, to release the encapsulated hydrophilic

compound in response to a change of pH media from 7 to 5 was demonstrated. More advanced research on pH-dependent rate and maximal release from the fliposomes was reported in [20]. In this study, the difference in rate and maximal release from individual fliposomes and fliposomes adsorbed on the polycationic particles was examined. Given that the amount/concentration of a trigger-lipid in the membrane also affects the pH-dependent release properties of the fliposomes [21], it is assumed that the membrane structure is significantly changed in the presence of a pH-sensitive trigger-lipid. This hypothesis was based on experiments that are sensitive to the microscopic structure of a lipid membrane. To shed light on the detailed molecular mechanism of membrane transformation, rigorous methods that can provide microscopic information about the release mechanism are needed.

Small-angle X-ray scattering (SAXS) and isothermal titration calorimetry (ITC) methods are known as powerful tools to study the membrane structure and release mechanism from fliposomes. These techniques were successfully applied to test a variety of phenomena in drug delivery systems at the microscopic scale. These include polymeric nanoparticles [22, 23, 24, 25], polymerosomes [26, 27, 28], liposomes [29, 30, 31].

In this work, SAXS and ITC measurements were carried out for the first time to deeply investigate the mechanisms that are involved in the process of hydrophilic model compound release from the inner cavity of anionic fliposomes at different pH values, temperatures and trigger-lipid amount. These methods were complemented by kinetic release studies.

2. Experimental Section

2.1. Materials

Reagents. Fumaryl chloride, dodecanol-1, butadiene sulfone, meta-chloroperoxybenzoic acid, morpholine were purchased from Sigma-Aldrich (St. Louis, MO, USA). Toluene, chloroform, dichloromethane, isopropyl alcohol, acetic acid,

sodium acetate, tris(hydroxymethyl)aminomethane were purchased from Reachim (Moscow, Russia).

Lipids. 1,2-Dioleoyl-*sn*-glycero-3-phosphocholine (PC), 1-palmitoyl-2-oleoyl-*sn*-glycero-3-phospho-L-serine (PS), and 1,2-dioleoyl-*sn*-glycero-3-phospho-(1-*rac*-glycerol) (PG) were purchased from Avanti Polar Lipids Inc (Alabaster, AL, USA). trans-4,5-Didodecyloxycarbonyl-2-morpholinocyclohexanol, trigger-lipid (TR), was synthesized as described elsewhere [17], the purity of the compound was confirmed by ^1H NMR (Figure S1, Supplementary Information). The chemical structures of investigated lipids are presented in Figure 1.

2.2. Methods

Preparation of fliposomes. Small unilamellar anionic fliposomes were prepared by the following procedure. Appropriate amount of lipid solutions in chloroform were mixed in a flask and then the solvent was evaporated under vacuum in a rotor evaporator Rotavapor (Buchi) at $36°C$. The thin film of the lipid mixture was then dispersed in a buffer by a disperser. Then the suspension of multilamellar fliposomes was dispersed with a 4700 Cole-Parmer ultrasonic homogenizer for 600 s (2×300 s) at 22 kHz above the membrane phase transition temperature. Liposomal samples were separated from titanium dust in a next step by centrifugation for 5 min at 11000 rpm using the centrifuge J-11 (Beckman). The molar fraction of PS (ν_{PS}) was 10% for all types of used fliposomes, while the molar fraction of trigger-lipid (ν_{TR}) varied from 10 to 40%.

Fliposomes loaded with NaCl solution were prepared by dispersing a lipid film in $1M$ NaCl solution in buffer ($10^{-3}M$) followed by dialysis against 1 L of $10^{-3}M$ buffer for 2 hours (2×1 h). The fliposomes concentration was recalculated after the dialysis according to the dilution of fliposomes during the dialysis (generally not more than 6%). Fliposomes were studied within 3 days from preparation.

Microelectrophoresis and dynamic light scattering (DLS). Light scattering and electrophoretic mobility was measured with the same Zetasizer Nano-ZS instru-

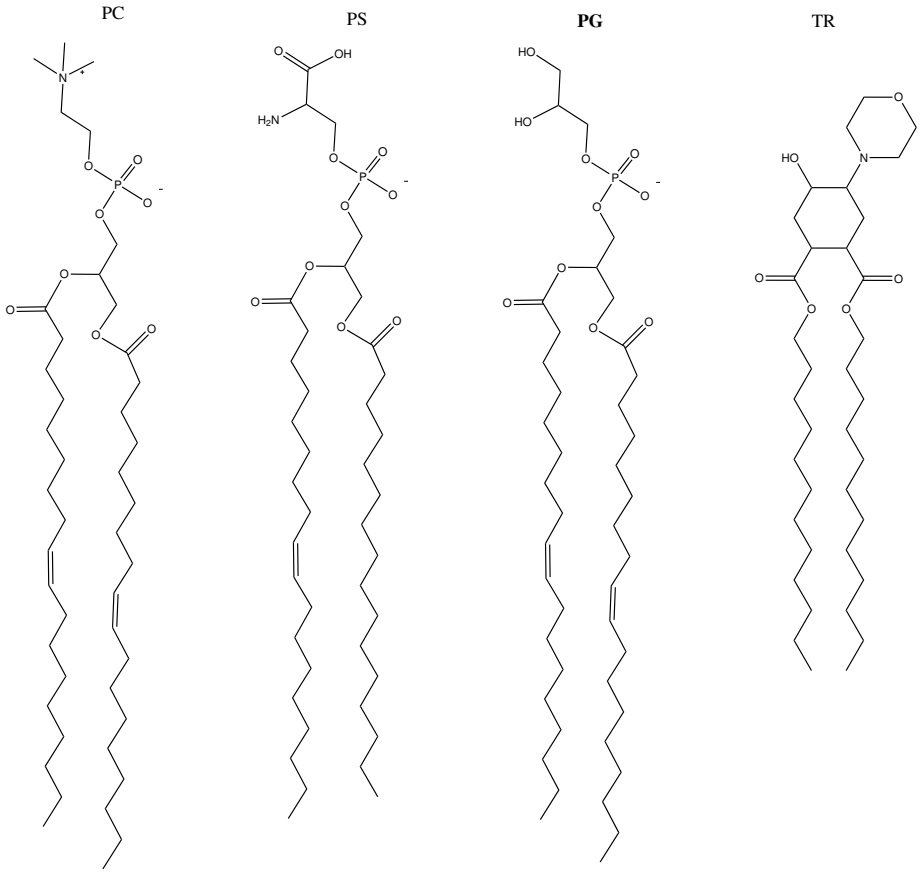

Figure 1: Schematic representation of the studied lipids: 1,2-Dioleoyl-*sn*-glycero-3-phosphocholine(PC), 1-palmitoyl-2-oleoyl-*sn*-glycero-3-phospho-L-serine(PS), 1,2-dioleoyl-*sn*-glycero-3-phospho-(1-*rac*-glycerol)(PG) and trans-4,5-Didodecyloxycarbonyl-2-morpholinocyclohexanol, trigger-lipid (TR).

ment used for dynamic light scattering measurements. The DTS software was used to compute zeta-potential values through the Henry equation (Eq.1). The electrophoretic mobility of a spherical particle is related to the zeta-potential by

$$U_E = (\zeta 2\epsilon_r f(ka))/3\eta \tag{1}$$

where ϵ_r is the dielectric constant of the sample, η is the dynamic viscosity (Pa s), and ζ is the zeta-potential (V); $f(ka)$ is Henry's function, which is calculated within the approximation of Smoluchowski ($f(ka) = 1.5$) for aqueous solutions of moderate ionic strength [32]. Each mobility value presented in the text is an average of 15 up to 100 values.

In the dynamic light scattering experiment, the hydrodynamic radius R_h of fliposomes was measured as a function of pH. A refractive index of 1.59 and an absorbance of 0.01 were used for all measurements. Viscosity (0.8872 cP) and refractive index (1.33) of water were used as dispersant parameters. The measurements were conducted in triplicate for 60 seconds per run, with 3 runs per measurement at $25°C$. The measurement angle was set to 173°. For the data processing, the normal resolution analysis model (general purpose algorithm) was selected [33].

Small-angle X-ray scattering (SAXS). SAXS experiments were performed on the B21 beam line (Diamond Light Source, Didcot, UK) with the fliposomes loaded with $1M$ solution of CsCl. The X-ray scattering images were recorded using a monochromatic incident X-ray beam ($\lambda = 1.54$ Å) covering the $0.04\ nm^{-1} < q < 4.0\ nm^{-1}$ range of a scattering vector ($q = 4\pi/\lambda \sin\theta$), with 2θ the scattering angle). The 2D scattering patterns were isotropic. They were azimuthally averaged to yield the dependence of the scattered intensity $I_s(q)$ on the scattering vector q. Prior to fitting analysis, the solvent scattering has been subtracted. Obtained SAXS curves were fitted with the "Bilayered vesicles" model using the SASFit software [34]. This model has the following fitting parameters (Figure 2). R – the radius of a core; t_H - thickness of the hydrophilic part of the bilayer; t_T - thickness of the hydrophobic part of the bilayer; ρH_2O - scattering length

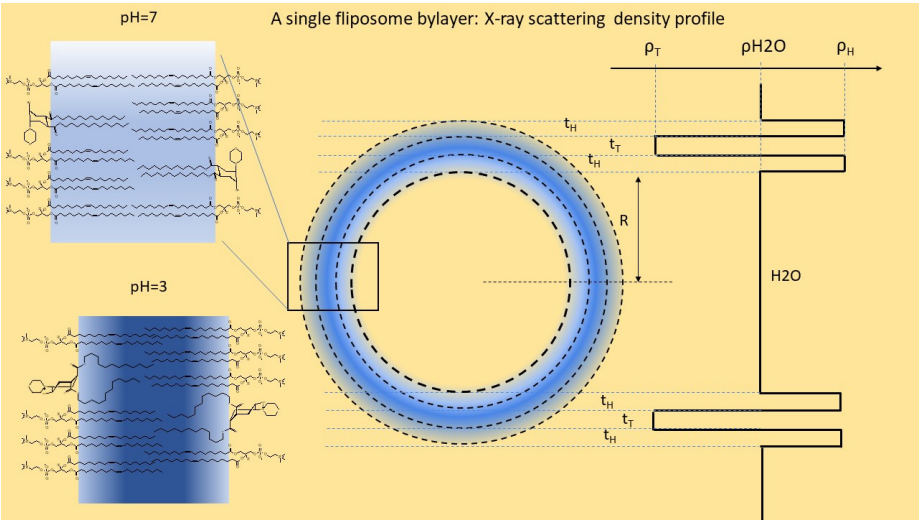

Figure 2: The suggested structure for liposome membranes (left) the liposome membrane structure at two extreme pH values; (middle) the bilayered vesicle model; (right) the vesicle scattering length density (SLD) profile across the membrane. R – the radius of the core; t_H - thickness of hydrophilic part of bilayer; t_T - thickness of the hydrophobic part of the bilayer; ρH_2O - scattering length density of solvent; ρ_H- scattering length density of the hydrophilic part of the bilayer; ρ_T - scattering length density of the hydrophobic part of the bilayer. The scattering length density of the solvent is fixed (9.44×10^{-6} Å^{-2}.)

density (SLD) of solvent; ρ_H- scattering length density of the hydrophilic part of the bilayer; ρ_T - scattering length density of the hydrophobic part of the bilayer. The scattering length density of the solvent was fixed (9.44×10^{-6} Å^{-2}).

Isothermal titration calorimetry (ITC). The microcalorimetry study was performed using a MicroCal iTC200 isothermal titration calorimeter. The experiment was performed with consecutive injections of the acid solution into the 280 μL calorimeter cell containing the liposome solution (5 mg/mL). An acid solution was added to a 40 μL injection syringe, the tip of which was modified to act as a stirrer. The chosen stirring speed was 1000 rpm. The injection volume varied and was 0.5, 1 and 2 μL in each experiment. The time between injections was of 200 s. The measurements were recorded at 30°C. The acid solution concentration in the syringe was dependent on the molar fraction of trigger-lipid

(ν_{TR}) and was 6, 9, 12.5, 16, and 25 mM for ν_{TR} = 10, 15, 20, 25, and 30% correspondingly. The data were analyzed using the Microcal Origin software. Experimental enthalpy values were obtained by integrating the raw data signal, and the integrated molar enthalpy change per injection was obtained by dividing the experimentally measured enthalpy values by the number of moles of the acid added. The final enthalpograms represent the intergrated molar enthalpy values as a function of equivalent of HCl to TR. The blank experiment of HCl titration into Mili-Q water was additionally performed in the same conditions to evaluate the HCl dissolution thermal effect.

Release kinetics measurement. Kinetic release experiments were performed for the 1 mg/mL suspension of fliposomes loaded with 1M NaCl. Fliposomes of different compositions (ν_{TR} = 10, 15, 20, 25, and 30%), at fixed pH 7 were transferred to buffer solutions of various final pH (3.36, 4.01, 4.39, 4.80, and 5.40) and release kinetic was monitored at different temperatures (25, 28, 31, 34, 37, and 40°C). The pH-induced release of NaCl from the inner cavity of fliposomes was followed by conductometry with a CDM83 conductometer (Radiometer, Copenhagen, Denmark). The cell temperature was maintained constant with an accuracy of 0.1°C.

3. Results and discussions

Before analysing and discussing the experimental results several features of the studied systems should be noted. The individual lipids used for the fliposomes preparation undergo a melting phase transition at different temperatures. The overall melting temperature for the particular fliposome system is governed by the lipid composition. Moreover, the membrane permeability is directly connected with the overall phase transition temperature of the membrane. The existence of the melting phase transition temperature resulted in some peculiarities we faced while preparing the fliposomes. With the increasing of trigger-lipid amount in the membrane, the temperature of ultrasound treatment had to be increased to ensure that fliposomes were formed. Thus, fliposomes with 10–20%

of trigger-lipid were sonicated at temperatures 10–20°C; 25–30% – at temperatures 25–30°C. And for fliposomes with 35-40% of trigger-lipid the ultrasonic treatment was processed at 60°C.

Another issue should be mentioned here. To gain the detailed picture of the metamorphoses that take place in the membrane structure with a change of pH, the knowledge about pKa values of all lipids is needed. Moreover, it is known that the pKa of the pH-sensitive component of the drug delivery container should be in the range of the target media pH value for the better therapeutic efficiency [35]. However, the pKa value for the trigger-lipid was reported in methanol only [18] due to its low water solubility; the reported pKa value in methanol was 4.6. Therefore, the determination of the pKa value for the trigger-lipid was essential for our study.

3.1. Trigger-lipid pKa determination

Therefore, the first step was to determine the pKa of the trigger-lipid in the fliposomal membrane formed in aqueous solution. We had to decipher a novel way to determine the pKa of the trigger-lipid in aqueous solution. The protonation process was followed by the determination of the fliposomes surface charge at different pH values. At alkaline pH values the trigger-lipid is not charged, however, with the decreasing of pH it protonates and acquires a positive charge [36]. Meanwhile, the fliposomes possess a negative charge due to the presence of anionic lipid at alkaline pH. At the pH values below 7.0 a significant change of the surface charge value was monitored. The presence of trigger-lipid in the membrane shifts the surface charge value as seen by electrophoretic mobility (EPM) values (Figure 3A). When the amount of protonated trigger-lipid reaches 10% mole, and equals the molar fraction of anionic lipid, the surface charge of fliposomes should be close to zero. The surface charge of the fliposomes was thus determined by transferring an aliquot of the fliposomal suspension into a buffer solution with a proper pH value.

As we expected, we observed the dependence of the pH value, at which the fliposomal suspension is neutral, on the molar fraction of trigger-lipid in

the membrane. The neutral surface charge means that the amount of cationic charges is equal to anionic. Having assumed that the cationic charge in the fliposomal membrane comes from the protonation of the trigger-lipid, we calculated the α value of trigger-lipid at a given pH corresponding to a neutral surface charge as:

$$\alpha = \nu_{PS}/\nu_{TR} \tag{2}$$

where α – degree of protonation of TR, ν_{PS} – molar fraction of anionic lipid (PS), ν_{TR} – molar fraction of trigger-lipid (TR).

The calculated α value for the fliposomes with different molar fractions of trigger-lipid was depicted as a function of pH (Figure S2A, Supplementary Information) and the pKa was calculated at the final stage. The obtained pKa value was 4.85, that is in a good agreement with the pKa value of the same trigger-lipid determined from NMR experiments in deuterated methanol – 4.6 [18].

However this approach has a flaw. PS molecule has three groups capable of protonation: phosphate (pKa = 2.6), carboxyl (pKa = 5.5) and amino (pKa = 11.55) [37]. As the pH value in our experiments varied from 3.0 to 9.0, the presence of carboxyl group in PS can interfere with trigger-lipid pKa determination. One can see, that for the trigger-free liposomes with only 10% of PS the surface charge neutralization occurs at pH values below 5.0 (Figure 3 A, curve 0%). Thus, in the presence of the trigger-lipid, both protonation of the trigger-lipid and PS takes place in a range of pHs 5–3 and as a result the obtained α values for trigger-lipid in fliposomes were overvalued, and thus the pKa value was, consequentially, undervalued.

To overcome this obstacle we have used another anionic lipid without a carboxyl group – phosphatidylglycerol (PG). PG has only one ionizable moiety – phosphate group of pKa value 3.5. PG protonates at pH values below 4 and its presence in the membrane should not interfere with the protonation of trigger-lipid at pH values above 4.0. Indeed, as seen on Figure 3B(10%), the EPM value for the fliposomes with 10% of trigger-lipid does not exceed zero as observed in

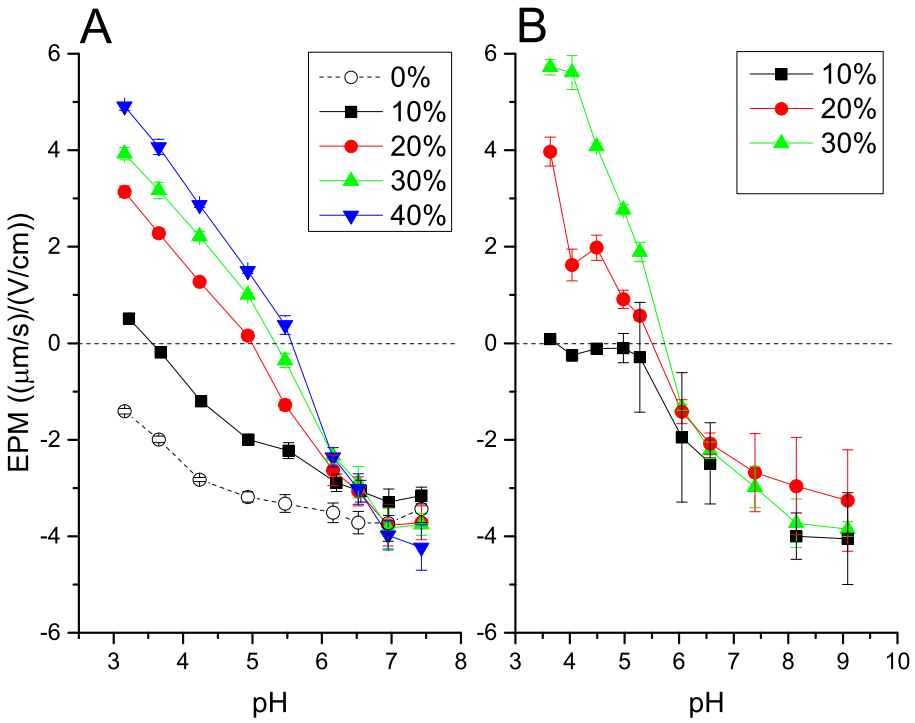

Figure 3: Electrophoretic mobility depenence of fliposomes with PS (A) and PG (B) on pH.

the corresponding curve on Figure 3A(10%).

Calculated α values were plotted as a function of pH values for the neutral fliposomes (Figure S2B, Supplementary Information) and approximated with a linear function. The correct value of trigger-lipid pKa determined by our approach was 5.55 and was drastically different from the previously reported value in methanol.

Thus we developed a novel way to determine pKa values in water media for non-soluble lipid in water.

3.2. Elucidation of the changes in the membrane structure

To monitor the possible structural changes in a fliposomal membrane we performed SAXS measurements for the 25% trigger-lipid and trigger-free fliposomes. Steady-state SAXS measurements were performed at various pH values

from 3 to 7 (Figure 4 A and B). Several features should be noted here. The intensity at the lowest q increases with decreasing pH for the system with 25% of trigger-lipid (Figure 4C). This might be an indication of either a particle size growth or an increase of the particles number. In contrast, there are just minor changes in the scattering intensity as a function of pH for the system with no trigger-lipid (Figure 4C). The correlation peak at high q values is also pH sensitive. Whereas it has a pronounced shape at acidic pH, it's barely visible in basic conditions (Figure 4 A and B). It's known that the correlation peak for liposomes occurs due to inverse scattering length densities for X-rays inside of a lipid membrane [38]. Such a correlation peak transformation implies paramount changes in the thicknesses and scattering length contrasts of hydrophobic and hydrophilic layers. Thus, visual inspection of SAXS curves at different pHs provides a clear evidence of structural changes in the fliposome membrane composed of 25% of trigger-lipid with decreasing of pH. Using the Bilayered vesicle model (Figure 2) we were able to fit all SAXS data.

The fitted values of hydrophobic, t_t, and hydrophilic, t_h, layers thickness are presented in Figure 5A. The thicknesses for the hydrophobic and hydrophilic layers for the control membrane (without trigger-lipid) liposomes show no dependence on the pH value and are of (24.9 ± 0.9) Å and (16.0 ± 0.6) Å, correspondingly, that is in a good agreement with the literature data [39]. However, the thicknesses of hydrophobic and hydrophilic layers of fliposomes with 25% of trigger-lipid do change with the variation of the pH value. Hydrophilic layer is getting thicker (from 16.2 to 21.3 Å) with the decreasing of the pH value (from 6.0 to 3.0) that could be related to the protonation of the trigger-lipid polar group. In contrast, the hydrophobic layer becomes thinner (from 27.3 to 21.1 Å) due to the shrinkage of the membrane thickness related to the change in trigger-lipid conformation. The total thickness of the fliposomal membrane slightly grows with the decrease of pH value – from 59.6 Å at pH 6.0 to 63.7 Å at pH 3.0 in comparison with with (57.0 ± 2.0) Å for the trigger-free liposomes.

The obtained values of vesicle sizes fitted from the SAXS data are in a good agreement with the ones obtained from dynamic light scattering (DLS) mea-

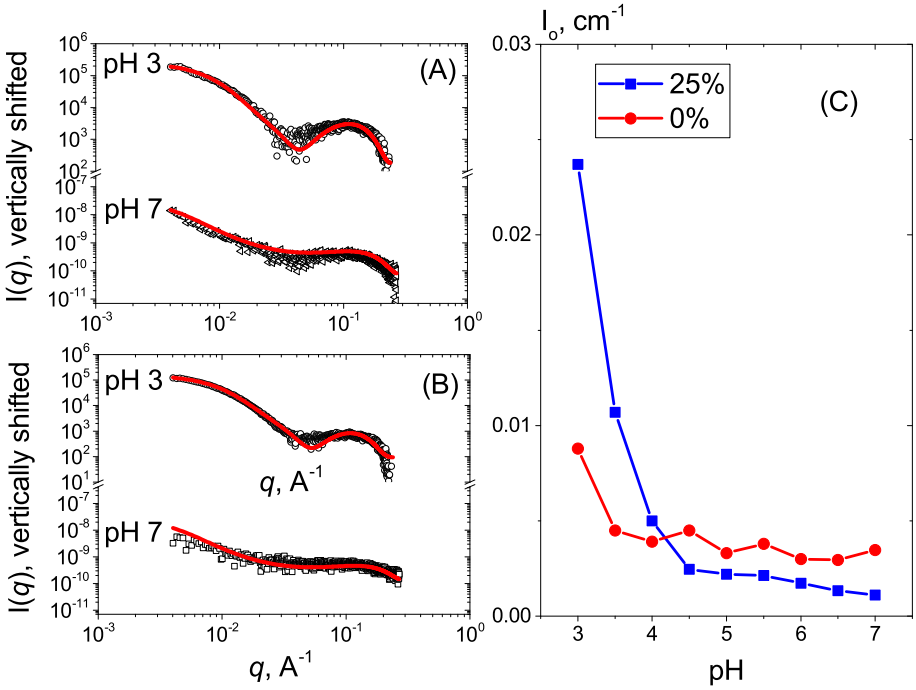

Figure 4: SAXS curves for 0% (A) and 25% (B) of trigger-lipid at pH values of 3 and 7. Red lines are fits of the scattering data with the model described in the experimental section. Curves are vertically shifted for clarity. (C) The scattering intensity at lowest q-value as a function of pH for 0% (red curve) and 25% (blue curve).

surements (Figure 5(B)). As the decrease in pH value induces a conformational switch of the trigger-lipid what disturbs the fliposomal membrane, it also can lead to the change in size due to aggregation or fusion of the fliposomes.

3.3. Fliposomes protonation study

Several simultaneous processes might take place when the fliposomes are in a media of acidic pH: 1) the protonation of trigger-lipid accompanied with a change of its conformation followed by lipid bilayer destabilisation and the formation of defects in a liposomal membrane; 2) the release of the hydrophilic content from fliposomes through the formed defects; and 3) defects self-healing due to the lateral diffusion of lipids.

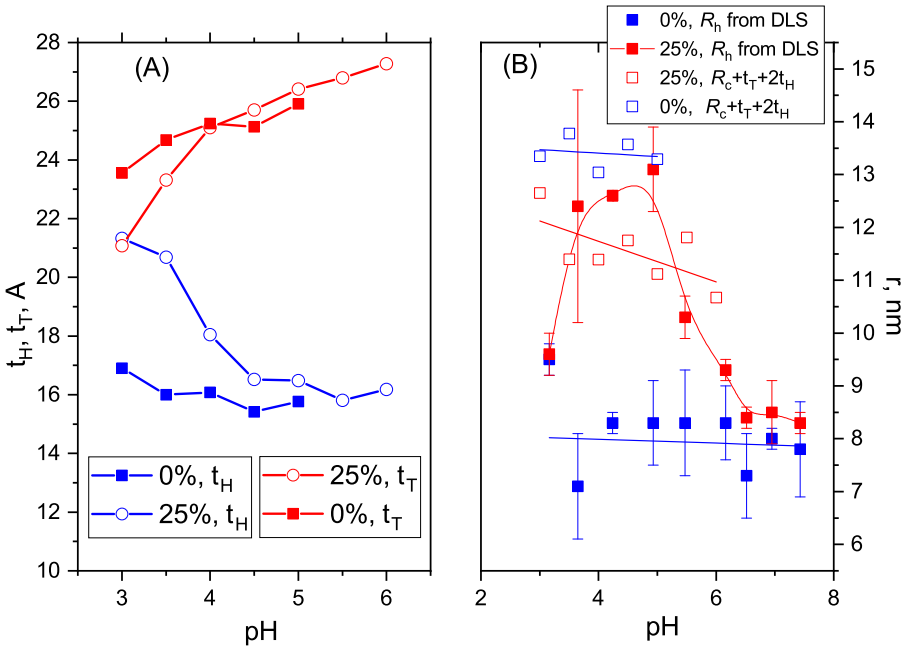

Figure 5: (A) Hydrophilic (t_h) and hydrophobic (t_t) layers thicknesses for control (without trigger-lipid) liposomes as a function of pH. (B) Radius of the core (open squares) and hydrodynamical radius (filled squares) as a function of pH.

To confirm the transformation of fliposome membranes observed in SAXS experiments we performed ITC experiments. The suspensions of fliposomes were titrated with an HCl solution with the proper concentration (Experimental section).

ITC experiments reveal that fliposomes protonation is exothermal (Figure 6A). The acidification of the fliposomal suspension, as mentioned above, reveals several processes, that can be attributed to individual contributions: protonation, the disturbance of the liposomal membrane due to the conformational change of the trigger-lipid, and the self-healing of the membrane. However, the differentiation of the individual contribution for each process to the overall thermal effect is beyond the scope of this paper. Thus, we made only qualitative conclusions from the ITC experiments. The enthalpy change as a function of equivalent [HCl]/[TR] shows a biphasic behavior. The exothermic effect in-

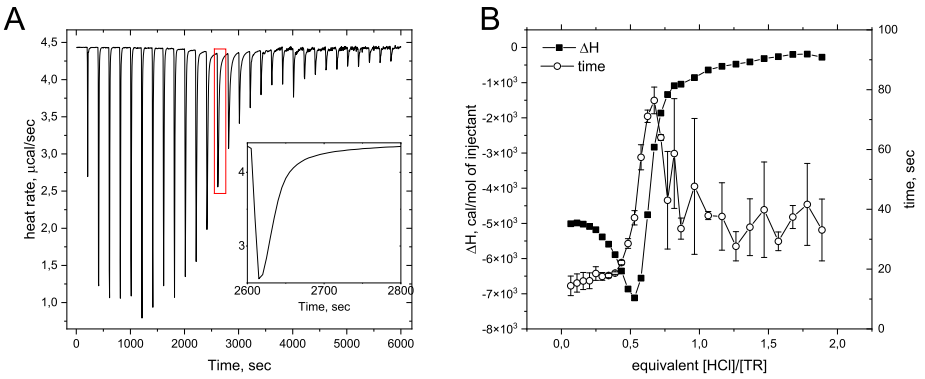

Figure 6: (A) ITC raw data (inset: slow decay process) and (B) enthalpogram and slow time decay as a function of equivalent [HCl]/[TR]. Fliposomes with 15% of trigger-lipid.

creases with increasing [HCl]/[TR] ratio reaching a well pronounced minimum at the value of 0.5. That precisely corresponds half of the trigger-lipid amount protonated in the fliposomes membrane. Even though we can't access the exact pH value of the minimum, we can attribute this process to the protonation of trigger-lipid. With further increasing of equivalent [HCl]/[TR] above 0.5, the delta H decreases and starts to be less exothermic (Figure 6B). We speculate that at 0.5 all trigger-lipids in the outer layer are protonated resulting in the transformation of both layers thicknesses that coexist with further protonation of the remaining trigger-lipid molecules. This complex behavior is revealed with the observed decrease in delta H values above 0.5. This hypothesis is based on the data obtained from the SAXS fitting (Figure 5). A similar biphasic behavior was observed with the other trigger-lipid content Figure S3. The only difference is the position of the minimum that could be explained by heterogeneous distribution of TR in the outer and inner layer of the membrane.

Another evidence of the membrane structural changes could be obtained from the analysis of ITC raw data. A slow decay process starts to be visible at equivalent [HCl]/[TR] = 0.5 (Figure 6A, inset), that corresponds to the range of the minimal value of the delta H. From the analysis with an exponential decay we were able to extract the decay times that are presented in Figure 6B. One can

see that the slowest decay time corresponds to the inflection point at equivalent [HCl]/[TR] = 0.7. We have attributed this kinetics to lipid layer rearrangement with changing pH.

3.4. Kinetics of release

Having obtained the evidence of membrane transformation as a function of pH, we focused on salt release studies.

The conductivity-time series was normalized using blank experiments by measurements with non-loaded fliposomal suspensions. The maximum value of conductivity was determined for salt-loaded fliposomes by disruption with Triton X-100 surfactant at each pH value. It is important to note that although the $1M$ NaCl solution creates a sufficiently high osmotic pressure within the liposome, the lipid membrane is strong enough to resist. Additional control experiments showed no salt leakage from the fliposomes at pH values above 6.5 (Figure S3, Supplementary Information).

Figure 7 represents the kinetic release curves for fliposomes with fixed amount of trigger-lipid at different pH values(A) and for fliposomes with different amount of TR at fixed pH value(B) and at fixed temperature.

The pH-induced release from fliposomes is affected by 3 factors: pH value of the media, molar fraction of TR, and temperature. Intuitively the release rate depends on the number of defects in a fliposomal membrane. The number of defects, in its turn, can be governed by adjusting the amount of the protonated trigger-lipid, either by varying the media pH (Figure 7A), or by changing the molar fraction of trigger-lipid in the membrane (Figure 7B).

As can be seen from the Figure 7, all kinetic release curves show a rapid growth followed by a plateau, reaching a steady-state value within 35 minutes.

In the majority of cases such kinetic profiles were fitted either by the initial slope calculation [20, 40, 41] or by a single or double exponential function [42]. The data obtained from such a fitting have no correlation with any physical parameters that are relevant to a particular liposomal system. No prediction can be made from the obtained release data. In this study we propose a novel

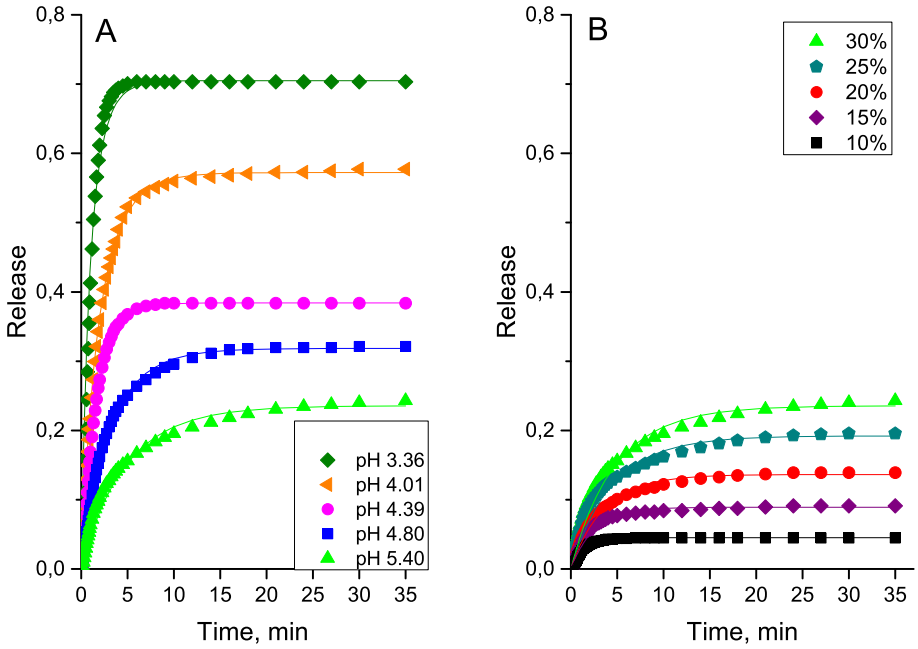

Figure 7: Kinetic release curves for (A) fliposomes 30% at different pH values and (B) fliposomes with different amount of trigger-lipid at fixed pH 5.40. The concentration of fliposomal suspension was set to 1 mg/mL. Temperature $37°C$. The solid lines are the fitting curves according to the equation 4.

model that is based on physico-chemical considerations of the release mechanism from fliposomes. Namely, for the first time we suggest a physical model that involves the mechanism of defects healing. The model assumes the formation of N_0 defects (pores) at the moment of stepwise pH change, with a release flow $\nu = k(C_{int} - C_{ext})$, where C_{int} and C_{ext} are the salt concentrations in the internal and external volume of the liposomes and k is the permeability constant. Once pores are formed, their amount decreases according to the first order kinetics: $N(t) = N_0 \exp(-t/T_r)$ where T_r is a self-healing time. In this case, the release flow at the time t could be written as:

$$\nu = kN_0(C_{int} - C_{ext}) \exp(-t/T_r) \tag{3}$$

The first derivative of the salt concentration over time in internal and external

space can be described as $dC_{int}/dt = -\nu/V_{int}$ and $dC_{ext}/dt = \nu/V_{ext}$ and $d(C_{int} - C_{ext})/dt = -\nu/(1/V_{int} + 1/V_{ext})$, where V_{int} and V_{ext} are the internal and external volumes of the liposomes.

By setting $x = C_{in} - C_{ext}$ and $A = 1/(1/V_{int} + 1/V_{ext})$ to constant values we can rewrite 3 as:

$$dx/dt = -AkN_0 \exp(-t/T_r)X$$

by setting initial conditions as $x(0) = C_0$, where C_0 is the initial salt concentration in the internal volume and the salt concentration in the external volume is 0 we can solve this differential equation as:

$$x(t) = C_0 \exp(AkN_0/T_r(\exp(-t/T_r) - 1))$$

Taking into account that measured release $R(t) = C_{ext}(t)/C_{ext}(\infty)$, the final kinetic release equation can be written as:

$$R(t) = 1 - \exp(AkN_0 \frac{\exp(-t/\tau_r) - 1}{\tau_r}) \quad (4)$$

, where τ_r - the self-healing time for a lipid layer, and kN_0 is the product of the pore concentration (N_0) and permeability (k) of each pore. Note, that both k and N_0 cannot be determined separately, only their product is observable.

The obtained values of self-healing rate ($1/\tau_r$) depend on the trigger-lipid content and pH value of the release experiment. These dependences are presented in Figure 8(B). It is clearly seen, that the membrane self-healing rate has a minimum on pH dependence, the position of this minimum depends on the trigger-lipid content. For 10% fliposomes the minimum is observed at pH $<$ 3.5 and shifts toward alkaline region with increasing trigger-lipid content. The minimum in self-healing rate reaches value $>$ 5.5 for 30% TR in the fliposomes. Such a trend is closely correlated with electrophoretic mobility data, Figure 3(A) – the minimum value of self-healing rate corresponds to pH values close to the zero-charge point of the fliposomes. The values of $1/\tau_r$ commonly increase with temperature increase, but keep the trend on pH dependence reaching a minimum at the isoelectric point of the lipid bilayer.

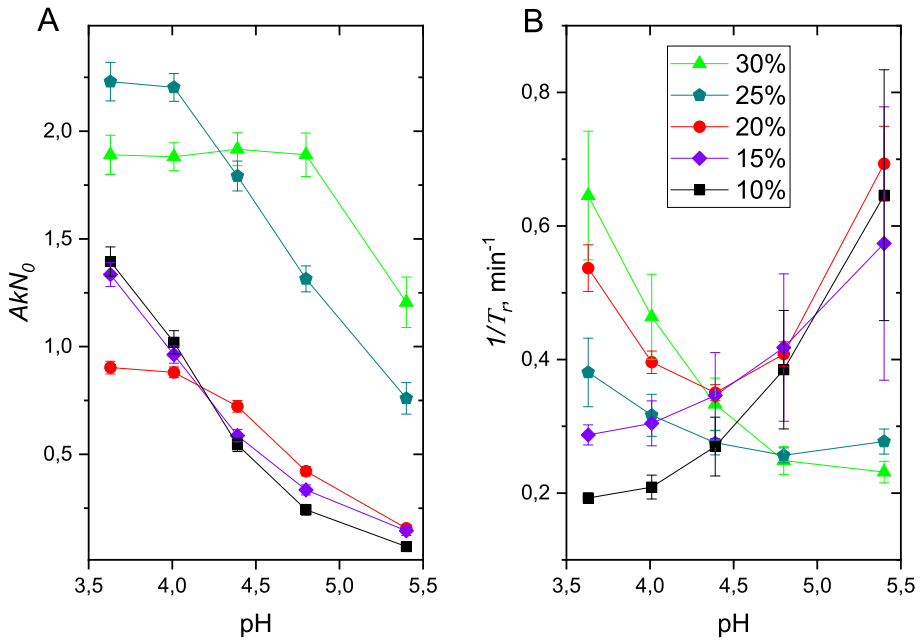

Figure 8: (A) kN_0 dependence on pH. (B) Self-healing rate ($1/\tau_r$) dependence on pH. Temperature 37°C. See equation 4 for parameters description.

The obtained self-healing time is (1.5 – 5 min) of the same order of magnitude higher that the ones observed by ITC. This is the indirect confirmation that the second process visualized by ITC can be attributed to self-healing events of the membrane. The discrepancy between both times is somewhat not surprising given the different sensitivity and nature of both experiments; ITC monitors the heat changes that occur during the membrane transformation with changing pH, whereas the release is a combination of several elementary events.

The dependence of kN_0 values (Figure 8(A)) on pH increases with lowering of pH corresponding to protonation of TR. At the lowest pH this value is almost constant, because all trigger-lipids was protonated.

4. Conclusions

In this paper we described a novel way to determine the pKa of trigger-lipid in a fliposomal membrane in water. The determined pKa (5.55) value

was significantly higher than the one obtained in methanol (4.6). With this knowledge better control over liposomal formulation can be achieved.

We gained numerous evidences that the fliposomal membrane is a subject of drastic alteration with changing pH. It was shown by SAXS experiments that the thickness of the membrane and the size of fliposomes are sensitive to pH values near the pKa of the trigger-lipid. These changes were additionally monitored by ITC that proves the existence of a biphasic process when the protonation is followed by lipid membrane transformation. We assume that the protonation takes place in the outer layer of the fliposomal membrane as the first step, followed by inner layer protonation resulting in membrane transformation.

We suggested for the first time a physical model of the drug release kinetics that is based on membrane structural parameters such as self-healing time and rate constant. Other models reported so far do not incorporate self-healing time as a fitting parameter. We were able successfully to fit all kinetic release data by the proposed model and extract valuable information on self-healing time and rate constant as function of trigger-lipid content, pH and temperature. It was observed that self-healing time is a non-monotonous function with an extreme point that is correlated with the trigger-lipid content, pH and temperature. Our model allows prediction of drug release rate and gives opportunity to design optimal liposomal formulations.

5. CRediT authorship contribution statement

Olga V. Zaborova: Conceptualization, Investigation, Methodology, Writing - Original Draft. **Vadim A. Timoshenko:** Software, Formal analysis, Writing - Original Draft. **Corine Nardin:** Resources, Writing - Review & Editing. **Sergey K. Fillipov:** Investigation, Methodology, Visualization, Writing - Original Draft.

6. Declaration of Competing Interest

The authors declare that they have no known competing financial interests or

personal relationships that could have appeared to influence the work reported in this paper.

7. Acknowledgements

This research was supported by the Russian Science Foundation (project 18-73-00076). Diamond Light Source (Didcot, UK) is acknowledged for beam time allocation (experiment SM12411-3).

References

[1] J. Zuegg, M. A. Cooper, Drug-likeness and increased hydrophobicity of commercially available compound libraries for drug screening, Current Topics in Medicinal Chemistry 12 (14) (2012) 1500–1513. doi:10.2174/156802612802652466.

[2] A. Lamprecht (Ed.), Nanotherapeutics. Drug Delivery Concepts in Nanoscience, Jenny Stanford Publishing, 2008. doi:10.1201/b11143.

[3] V. P. Torchilin, Recent advances with liposomes as pharmaceutical carriers, Nature Reviews Drug Discovery 4 (2) (2005) 145–160. doi:10.1038/nrd1632.

[4] N. Filipczak, J. Pan, S. S. K. Yalamarty, V. P. Torchilin, Recent advancements in liposome technology, Advanced Drug Delivery Reviews 156 (2020) 4–22. doi:10.1016/j.addr.2020.06.022.

[5] D. Guimarães, A. Cavaco-Paulo, E. Nogueira, Design of liposomes as drug delivery system for therapeutic applications, International Journal of Pharmaceutics 601 (2021) 120571. doi:10.1016/j.ijpharm.2021.120571.

[6] A. Akbarzadeh, R. Rezaei-Sadabady, S. Davaran, S. Joo, N. Zarghami, Y. Hanifehpour, M. Samiei, M. Kouhi, N.-K. K., Liposome: classification, preparation, and applications, Nanoscale research letters 8 (2013) 1–9.

[7] L. Sercombe, T. Veerati, F. Moheimani, S. Y. Wu, A. K. Sood, S. Hua, Advances and challenges of liposome assisted drug delivery, Frontiers in Pharmacology 6 (2015) 286. doi:10.3389/fphar.2015.00286.

[8] E. S. Lee, Z. Gao, Y. H. Bae, Recent progress in tumor ph targeting nanotechnology, Journal of controlled release 132 (3) (2008) 164–170. doi:10.1016/j.jconrel.2008.05.003.

[9] L. Tian, Y. H. Bae, Cancer nanomedicines targeting tumor extracellular ph, Colloids and Surfaces B: Biointerfaces 99 (2012) 116–126, smart Biointerfaces. doi:10.1016/j.colsurfb.2011.10.039.

[10] S. Filippov, M. Hrubý, v. Koňák, H. Macková, M. Špirková, P. Štěpánek, Novel ph-responsive nanoparticles, Langmuir 24 (17) (2008) 9295–9301. doi:10.1021/la801472x.

[11] S. K. Filippov, P. Chytil, P. V. Konarev, M. Dyakonova, C. M. Papadakis, A. Zhigunov, J. Plestil, P. Stepanek, T. Etrych, K. Ulbrich, D. I. Svergun, Macromolecular hpma-based nanoparticles with cholesterol for solid-tumor targeting: Detailed study of the inner structure of a highly efficient drug delivery system, Biomacromolecules 13 (8) (2012) 2594–2604. doi:10.1021/bm3008555.

[12] L. Liu, W. Yao, Y. Rao, X. Lu, J. Gao, ph-responsive carriers for oral drug delivery: challenges and opportunities of current platforms, Drug Delivery 24 (1) (2017) 569–581. doi:10.1080/10717544.2017.1279238.

[13] B. C. Garcia, D. Shi, T. Webster, Tat-functionalized liposomes for the treatment of meningitis: an in vitro study, International Journal of Nanomedicine 12 (2017) 3009–3021. doi:10.2147/IJN.S130125.

[14] W. Wu, L. Luo, Y. Wang, Q. Wu, H.-B. Dai, J.-S. Li, C. Durkan, N. Wang, G.-X. Wang, Endogenous ph-responsive nanoparticles with programmable size changes for targeted tumor therapy and imaging applications, Theranostics 8 (2018) 3038–3058. doi:10.7150/thno.23459.

[15] V. Passos Gibson, M. Fauquignon, E. Ibarboure, J. Leblond Chain, J.-F. Le Meins, Switchable lipid provides ph-sensitive properties to lipid and hybrid polymer/lipid membranes, Polymers 12 (3). doi:10.3390/polym12030637.

[16] A. V. Samoshin, I. S. Veselov, V. A. Chertkov, A. A. Yaroslavov, G. V. Grishina, N. M. Samoshina, V. V. Samoshin, Fliposomes: new amphiphiles based on trans-3,4-bis(acyloxy)-piperidine able to perform a ph-triggered conformational flip and cause an instant cargo release from liposomes, Tetrahedron Letters 54 (41) (2013) 5600–5604. doi:10.1016/j.tetlet.2013.07.156.

[17] B. Brazdova, N. Zhang, V. V. Samoshin, X. Guo, trans-2-aminocyclohexanol as a ph-sensitive conformational switch in lipid amphiphiles, Chemical Communications (2008) 4774–4776doi:10.1039/B807704E.

[18] Y. Zheng, X. Liu, N. M. Samoshina, V. V. Samoshin, A. H. Franz, X. Guo, Fliposomes: trans-2-aminocyclohexanol-based amphiphiles as ph-sensitive conformational switches of liposome membrane – a structure-activity relationship study, Chemistry and Physics of Lipids 210 (2018) 129–141. doi:10.1016/j.chemphyslip.2017.10.004.

[19] A. A. Yaroslavov, A. V. Sybachin, O. V. Zaborova, V. A. Migulin, V. V. Samoshin, M. Ballauff, E. Kesselman, J. Schmidt, Y. Talmon, F. M. Menger, Capacious and programmable multi-liposomal carriers, Nanoscale 7 (2015) 1635–1641. doi:10.1039/C4NR06037G.

[20] A. V. Sybachin, O. V. Zaborova, K. M. Imelbaeva, V. V. Samoshin, V. A. Migulin, F. A. Plamper, A. A. Yaroslavov, Effects of the electrostatic complexation between anionic ph-sensitive liposomes and star-shaped polycations on the release of the liposomal content, Mendeleev Communications 26 (4) (2016) 276–278. doi:10.1016/j.mencom.2016.07.002.

[21] A. Y. Lokova, O. V. Zaborova, Modification of fliposomes with a polycation can enhance the control of ph-induced release, International Journal of Nanomedicine 14 (2019) 1039–1049. doi:10.2147/IJN.S190306.

[22] C. E. Blanchet, D. I. Svergun, Small-angle x-ray scattering on biological macromolecules and nanocomposites in solution, Annual Review of Physical Chemistry 64 (1) (2013) 37–54. doi:10.1146/annurev-physchem-040412-110132.

[23] A. Bogomolova, S. Keller, J. Klingler, M. Sedlak, D. Rak, A. Sturcova, M. Hruby, P. Stepanek, S. K. Filippov, Self-assembly thermodynamics of ph-responsive amino-acid-based polymers with a nonionic surfactant, Langmuir 30 (38) (2014) 11307–11318. doi:10.1021/la5031262.

[24] S. K. Filippov, A. Papagiannopoulos, A. Riabtseva, S. Pispas, Adsorption of lysozyme on ph-responsive pnba-b-paa polymeric nanoparticles: studies by stopped-flow saxs and itc, Colloid and Polymer Science 296 (7) (2018) 1183–1191. doi:10.1007/s00396-018-4329-4.

[25] B. Angelov, A. Angelova, S. K. Filippov, M. Drechsler, P. Štěpánek, S. Lesieur, Multicompartment lipid cubic nanoparticles with high protein upload: Millisecond dynamics of formation, ACS Nano 8 (5) (2014) 5216–5226. doi:10.1021/nn5012946.

[26] S. Lecommandoux, R. Borsali, M. Schappacher, A. Deffieux, T. Narayanan, C. Rochas, Microphase separation of linear and cyclic block copolymers poly(styrene-b-isoprene): Saxs experiments, Macromolecules 37 (5) (2004) 1843–1848. doi:10.1021/ma035627r.

[27] C. Sanson, O. Diou, J. Thévenot, E. Ibarboure, A. Soum, A. Brûlet, S. Miraux, E. Thiaudiére, S. Tan, A. Brisson, V. Dupuis, O. Sandre, S. Lecommandoux, Doxorubicin loaded magnetic polymersomes: Theranostic nanocarriers for mr imaging and magneto-chemotherapy, ACS Nano 5 (2) (2011) 1122–1140. doi:10.1021/nn102762f.

[28] W. Agut, A. Brûlet, C. Schatz, D. Taton, S. Lecommandoux, ph and temperature responsive polymeric micelles and polymersomes by self-assembly of poly[2-(dimethylamino)ethyl methacrylate]-b-poly(glutamic acid) double hydrophilic block copolymers, Langmuir 26 (13) (2010) 10546–10554. doi:10.1021/la1005693.

[29] O. V. Zaborova, S. K. Filippov, P. Chytil, L. Kováčik, K. Ulbrich, A. A. Yaroslavov, T. Etrych, A novel approach to increase the stability of liposomal containers via in prep coating by poly[n-(2-hydroxypropyl)methacrylamide] with covalently attached cholesterol groups, Macromolecular Chemistry and Physics 219 (7) (2018) 1700508. doi:10.1002/macp.201700508.

[30] C. Vargas, R. C. Arenas, E. Frotscher, S. Keller, Nanoparticle self-assembly in mixtures of phospholipids with styrene/maleic acid copolymers or fluorinated surfactants, Nanoscale 7 (2015) 20685–20696. doi:10.1039/C5NR06353A.

[31] A. D. Tsamaloukas, S. Keller, H. Heerklotz, Uptake and release protocol for assessing membrane binding and permeation by way of isothermal titration calorimetry, Nature Protocols 2 (2007) 695–704. doi:10.1038/nprot.2007.98.

[32] R. J. Hunter, Chapter 3 - the calculation of zeta potential, in: R. J. Hunter (Ed.), Zeta Potential in Colloid Science, Academic Press, 1981, pp. 59–124. doi:https://doi.org/10.1016/B978-0-12-361961-7.50007-9.
URL https://www.sciencedirect.com/science/article/pii/B9780123619617500079

[33] S. W. Provencher, A constrained regularization method for inverting data represented by linear algebraic or integral equations, Computer Physics Communications 27 (1982) 213–227. doi:10.1016/0010-4655(82)90173-4.

[34] I. Breßler, J. Kohlbrecher, A. F. Thünemann, *SASfit*: a tool for small-angle scattering data analysis using a library of analytical expressions, Journal of Applied Crystallography 48 (5) (2015) 1587–1598. doi:10.1107/S1600576715016544.

[35] M. Jayaraman, S. M. Ansell, B. L. Mui, Y. K. Tam, J. Chen, X. Du, D. Butler, L. Eltepu, S. Matsuda, J. K. Narayanannair, K. G. Rajeev, I. M. Hafez, A. Akinc, M. A. Maier, M. A. Tracy, P. R. Cullis, T. D. Madden, M. Manoharan, M. J. Hope, Maximizing the potency of sirna lipid nanoparticles for hepatic gene silencing in vivo, Angewandte Chemie International Edition 51 (34) (2012) 8529–8533. doi:10.1002/anie.201203263.

[36] P. N. Veremeeva, I. V. Grishina, O. V. Zaborova, A. D. Averin, V. A. Palyulin, Synthesis of 3,7-diacyl-1,5-dimethyl-3,7-diazabicyclo[3.3.1]nonane derivatives as promising lipid bilayer modifiers, Tetrahedron 75 (33) (2019) 4444–4450. doi:10.1016/j.tet.2019.06.009.

[37] A. P. Lipids. Ionization constants of phospholipids [online] (2022).

[38] E. Di Cola, I. Grillo, S. Ristori, Small angle x-ray and neutron scattering: Powerful tools for studying the structure of drug-loaded liposomes, Pharmaceutics 8 (2). doi:10.3390/pharmaceutics8020010.

[39] B. A. Lewis, D. M. Engelman, Lipid bilayer thickness varies linearly with acyl chain length in fluid phosphatidylcholine vesicles, Journal of Molecular Biology 166 (2) (1983) 211–217. doi:10.1016/S0022-2836(83)80007-2.

[40] O. Zaborova, Determination of kinetic parameters of salt release from solid anionic fliposomes, Russian Journal of General Chemistry 90 (4) (2020) 762–766. doi:10.1134/S1070363220040349.

[41] P. N. Veremeeva, O. V. Zaborova, I. V. Grishina, D. V. Makeev, V. A. Timoshenko, V. A. Palyulin, Stimulus-sensitive liposomal delivery system based on new 3,7-diazabicyclo[3.3.1]nonane derivatives, Bioorganic and Medicinal Chemistry Letters 39 (2021) 127871. doi:10.1016/j.bmcl.2021.127871.

[42] S. Modi, B. D. Anderson, Determination of drug release kinetics from nanoparticles: Overcoming pitfalls of the dynamic dialysis method, Molecular Pharmaceutics 10 (8) (2013) 3076–3089. doi:10.1021/mp400154a.